JOURNAL OF AGRICULTURAL AND FOOD CHEMISTRY

Transport of Commercial Endosulfan through a Column of Aggregated Vineyard Soil by a Water Flux Simulating Field Conditions

M. CARMEN LÓPEZ-BLANCO,† BEATRIZ CANCHO-GRANDE,† JESÚS SIMAL-GÁNDARA,*,† EUGENIO LÓPEZ-PERIAGO,‡ AND MANUEL ARIAS-ESTÉVEZ‡

Nutrition and Bromatology Group, Analytical and Food Chemistry Department, Soil and Agricultural Science Group, Plant Biology and Soil Science Department, Faculty of Food Science and Technology, University of Vigo, Ourense Campus, 32004 Ourense, Spain

Endosulfan is a potentially harmful, degradation resistant pesticide that is found in soils where it has been used. Despite being hydrophobic and having high affinity for soil matrix components, it has also been found in groundwater. To investigate this behavior, we studied the passage of a commercial emulsified formulation through a column of aggregated vineyard soil under simulated light rain. Breakthrough data were obtained using gas chromatography with electron capture detection to determine the concentration of endosulfan in samples extracted from the column periodically at several depths. These data, and analogous data obtained previously for the passage of bromide, were analyzed using the program CXTFIT v.2. Analysis of the bromide data strongly suggested the existence of preferential flow paths in the column. The endosulfan data were adequately accounted for by a model in which the preferential flow and nonpreferential flow regions are almost isolated from each other. These regions differ also as regards both the partition of endosulfan between soil and soil solution and the rate at which reversibly adsorbed endosulfan is transformed into irreversibly adsorbed endosulfan. The "irreversibility" sink term accounts also for biological and chemical degradation of endosulfan. The findings imply that soil humidity favors the transport of commercial endosulfan by the formation and maintenance of preferential flow paths in soil, controlling both the presence of endosulfan in groundwater and its high persistence in soil.

KEYWORDS: Soil transport; environmental fate; endosulfan; gas chromatography-electron capture detection

INTRODUCTION

A proportion of vineyard pesticide generally ends up in the soil, borne either in droplets of the pesticide spray that drift down onto the ground or in drops of rainwater that drip off the treated vine. This local contamination can spread more widely in the environment as the result of the deposited pesticide running off in stormwater or irrigation water, percolating through the soil, and reaching groundwater, or otherwise migrating from the site of application (*1*, *2*).

α-Endosulfan (6,7,8,9,10,10-hexachloro-1,5,5a,6,9,9a-hexahydro-6,9-methano-2,4,3-benzodioxathiepin-3-oxide) is a pesticide that is applied to the leaves of grapevines to keep infestation with vine leaf blister mite (*Eriophyes vitis*) below economically damaging levels. It is suspected of being carcinogenic and/or an endocrine system disrupter (*3*). It is hydrophobic, resistant to biotic and abiotic degradation under environmental conditions, and is found in groundwater and agricultural soils the world over (*4*−*9*). In the area in which the study described in this paper was carried out (in which endosulfan is used in the form of 0.15−0.30% solutions of Fosulan, a 35% endosulfan emulsion stabilized with surfactant), measurements in rainfall dripping through vineyard canopies suggest that the proportion of applied pesticide entering the soil in this way can reach 5% (*10*), and traces of endosulfan (0.02−0.06 μg/L) are found in 30% of drainage canals and wells (unpublished data).

Because the solubility of endosulfan in water is very low (≤0.5 mg/L) and its susceptibility to adsorption onto soil matrix components is high (K_{oc} = 350−1135) (*11*), it may be hypothesized that its presence in groundwater is due, as in the case of other pesticides (*12*), to transport from the surface down preferential flow paths, which can arise both in well-structured clay soils (*13*) and in poorly structured sandy soils (*14*). In this work, we tested this hypothesis by studying the passage of an

* To whom correspondence should be addressed. Tel: 34 988 387 060. Fax: 34 988 387 001. E-mail: jsimal@uvigo.es.
† Analytical and Food Chemistry Department.
‡ Plant Biology and Soil Science Department.

10.1021/jf050545i CCC: $30.25
Published on Web 07/28/2005

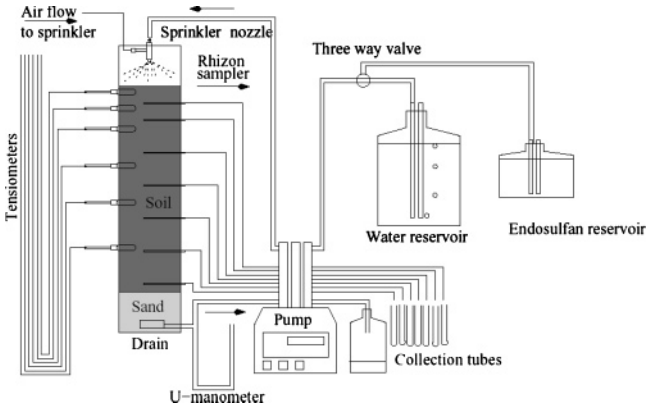

Figure 1. Experimental setup for monitoring endosulfan transport through a column of vineyard soil aggregates.

endosulfan pulse through a column packed with vineyard soil aggregates and maintained under uniform simulated rain.

MATERIAL AND METHODS

Soil. A sample was taken, with the least possible structural disruption, from the top 25 cm of the granitic, sandy loam soil of a vineyard in San Amaro (Arnoia, Ourense, Spain), and after it was dried in air, the 2−5 mm fraction was obtained by passage through appropriate sieves. The characteristics of this fraction, as determined from five replicate subsamples, were as follows: clay, 10.6 ± 0.4%; silt, 16.8 ± 0.6%; sand, 72.6 ± 0.7%; pH in water, 5.9 ± 0.2; pH in KCl, 4.9 ± 0.2; organic matter, 2%; nitrogen, 0.11 ± 0.01%; C/N ratio, 11 ± 1; cation exchange capacity, 2.1 ± 0.3 cmol/kg.

Column Setup. A drainage tube was placed in the bottom of a 15 cm i.d. PVC cylinder 80 cm long and was covered to a height of 9 cm with washed quartz sand particles sized 0.25−0.50 mm. The soil fraction described above was then introduced until the total height of solids was 59 cm (9 cm of sand plus 50 cm of soil), care being taken to avoid stratification or the disruption of aggregates (**Figure 1**). Microtensiometers were introduced into the soil column at depths of 1, 5.5, 10.5, 19.5, 28.5, and 38 cm from the surface and horizontal Rhizon leachate sampling probes (Eijkelkamp Agrisearch Equipment, Giesbeek, The Netherlands) at depths of 4, 8, 16, 24, 32, 40, and 48 cm. During experiments, a sprinkler head above the column that was connected to an air pump applied solutions that were pumped from their reservoirs by a Gilson Minipuls 3 multichannel peristaltic pump equipped with fluoroelastomer pumping tube, which was also used to pump leachate continuously from the drainage tube via 1 mm i.d. PTFE tubing and from the sampling probes via 0.5 mm i.d. PTFE tubing. A water-filled U-tube vacuum gauge was connected to the drainage tube to check that there was no suction at the bottom of the column (**Figure 1**).

Once the column had been set up and instrumentalized, it was sprinkled for 5 days with 5 L of 0.01 M KCl to control the ionic strength of the soil solution. At this point, a further 100 g of soil was added to compensate for settling, bringing the total weight of soil to 11.445 kg, its overall bulk density to 1.294 kg/L, and its porosity (v/v) to 0.486. Sprinkling with 0.01 M KCl solution was then continued for a further 2 days, during which the flow regime was brought to a steady 90 mL/h. The stationarity of the flow regime was checked by periodically weighing the column and measuring the volume of liquid pumped from the drainage tube and the sampling tubes (total for the seven, 7.00 ± 0.03 mL/h), and the tensiometers were periodically read to check the absence of matrix potential gradients (suction in all tensiometers was always greater than −0.5 cm of the water column). The volumetric water content θ was measured as 0.445, and the average velocity of flow through pores, v, was calculated therefrom as 1.14 cm/h.

Experimental Procedure. Once a stationary flow regime had been established in the column, it was sprinkled for 66 min with 25 mmol/L KBr solution, after which sprinkling of 0.01 M KCl solution was resumed and continued until the solute pulse had passed through the column. When passage was complete (which was deemed to have occurred after 60 h), the column was sprayed for 66 min with an aqueous solution of Fosulan with an α-endosulfan concentration of 100 mg/L, after which sprinkling of 0.01 M KCl solution was continued for 19 days. During all this time, the sprinkling rate of 90 mL/h was maintained. The accumulated samples from the lateral sampling tubes were removed for analysis hourly in the KBr experiment (sample volume 1.5 mL) and daily in the endosulfan experiment (sample volume 5 mL; in this case, 5 μL of a 70 mg/L solution of lindane in methanol was added to each sample as internal standard to correct for variability in analytical extraction efficiency, etc., and the samples were stored at <4 °C pending analysis).

Determination of Br^-. Br^- concentrations were determined by measuring the absorbance of tetrabromofluorescein at 520 nm (*15*) in an Auto Analyzer 3 segmented flow analyzer (Bran+Luebbe GmbH, Norderstedt, Germany). Recovery was 99.5%, and repeatability was 0.2%.

Determination of α-Endosulfan. *Chemicals and Standards.* α-Endosulfan [959-98-8] and lindane [58-89-9], both >98% pure, were obtained from Dr. Ehrenstorfer GmbH (Augsburg, Germany) and Aldrich (Milwaukee, MI), respectively. Methanol was purchased from Aldrich (Steinheim, Germany), ethyl acetate and potassium bromide were purchased from Merck (Darmstadt, Germany), and anhydrous sodium sulfate was purchased from Panreac (Barcelona, Spain). Water was obtained from a Waters Milli-Q system (Mildford, MA).

A stock standard solution of α-endosulfan in methanol with a concentration of ca. 1000 mg/L was prepared by weighing approximately 0.025 g of the analyte into a 25 mL volumetric flask and making up to volume, and working solutions with concentrations of 10 mg/L were prepared by dilution with methanol. A stock standard solution of lindane in methanol with a concentration of ca. 1000 mg/L was prepared by weighing approximately 0.01 g into a 10 mL volumetric flask and making up to volume, and working solutions with concentrations of 70 mg/L were prepared by dilution with methanol. Calibration standards were prepared by spiking 5 mL of water with 0.5, 2.5, 5.0, 10.0, or 15.0 μL of the working solution of endosulfan and 5 μL of the working solution of lindane. All standards were stored in the dark at 4 °C and used within 1 month, by which time they had undergone no degradation.

Extraction. A 5 mL volume of sample (spiked with lindane as described under Experimental Procedure) was placed in a 10 mL glass vial, 1 mL of ethyl acetate was added, and the vial was then sealed with Teflon-faced septa, shaken for 2 min, and left to stand upright for 3 min. The organic phase was drawn off and placed into a 350 μL insert in a 2 mL vial (from Supelco, Bellefonte, PA), where it was stored pending chromatography.

Chromatography. Chromatography of 1 μL samples was performed in a Fisons GC 8000 series gas chromatograph equipped with an electron capture detection system and with a Supelco MDN-5S 30 m × 0.25 mm i.d. fused silica capillary column with a 0.25 μm 5:95 diphenyl/dimethylsiloxane film. The oven temperature started at 80°, rose at 15 °C/min to 250 °C, and then at 5 °C/min to 300 °C, where it remained for 10 min. Injection was performed in split/splitless mode with 1 min splitless and a split ratio of 1/100; the injection temperature was 250 °C. The carrier gas was helium at a pressure of 125 kPa, and the detector makeup gas was nitrogen at 150 kPa. The detector temperature was 300 °C, and the current was set at 1 nA for a pulse voltage of 50 V.

Quantitation and Method Performance. For quantitation, a five-point calibration line was constructed using the ratio of the endosulfan and lindane peaks as dependent variables. Linearity (r^2) was better than 0.998 over the range 1−30 μg/L. The average recovery from seven 5 mL aliquots of Milli-Q water spiked with 2.0 μg/L of endosulfan (and with lindane as described under Experimental Procedure) was 75%, with a relative standard deviation of 7.8%.

Two-Region Transport Model. The hypotheses that there were preferential flow paths in the column, and that this preferential flow could account for the passage of endosulfan, were examined by investigating whether the bromide and endosulfan breakthrough data could be fitted by a two-region solute transport model (*16*). In this model, the soil solution is treated as divided between immobile and mobile regions. It is assumed that solutes infiltrate the soil from the

surface by diffusion and convection in the mobile region and by a first-order process of transfer from the mobile to the immobile region and that "reactive solutes" (in this work, endosulfan) undergo both reversible adsorption onto the soil matrix and a decay process (in this work, the decay process was interpreted as irreversible adsorption together with biological and/or chemical degradation of endosulfan in the 3 week duration of the experiment). These assumptions lead to the equations

$$(\theta_m + f\rho_b K_d)\,\partial c_m/\partial t = \theta_m(D_m\,\partial^2 c_m/\partial x^2 - v_m\,\partial c_m/\partial x) - \alpha(c_m - c_{im}) - (\theta_m \mu_{l,m} + f\rho_b K_d \mu_{s,m})c_m \quad (1)$$

$$[\theta_{im} + (1-f)\rho_b K_d]\,\partial c_{im}/\partial t = \alpha(c_m - c_{im}) - [\theta_{im}\mu_{l,im} + (1-f)\rho_b K_d \mu_{s,im}]c_{im} \quad (2)$$

where x is distance down the column (cm); t is time (h); the subscripts m and im indicate quantities describing the mobile and immobile liquid regions, respectively; c is concentration of solute (mg/L); θ_m and θ_{im} are the volumetric water contents of the soil in the mobile and immobile regions, respectively (L/L; both relative to the whole soil volume, so that $\theta_m + \theta_{im} = \theta$); v_m is the average velocity of water through pores in the mobile region (cm/h; $v_m = v\theta/\theta_m$); D_m is the hydrodynamic coefficient of dispersion of the solute in the soil solution in the mobile region (cm^2/h); α (h^{-1}) is the first-order mass transfer coefficient for solute exchange between the mobile and the immobile regions; f is the fraction of adsorption sites exposed to the mobile liquid phase; ρ_b is the bulk density of the solid phase; K_d (L/kg) is the partition coefficient for distribution of the solute between the solid and the liquid phases; and μ_l and μ_s (h^{-1}) are first-order rate constants for the decay of the solute in the liquid and solid phases, respectively. The corresponding equations for a solute that neither decays nor interacts with the soil (in this work, Br^-) are obtained by setting $K_d = \mu_{l,im} = \mu_{l,m} = \mu_{s,im} = \mu_{s,m} = 0$.

Equations 1 and 2 may be expressed in terms of dimensionless quantities in the form

$$\beta R\,\partial c_m/\partial T = (1/P)\,\partial^2 c_m/\partial Z^2 - \partial c_m/\partial Z - \omega(c_m - c_{im}) - \mu_m c_m \quad (3)$$

$$(1-\beta)R\,\partial c_{im}/\partial T = \omega(c_m - c_{im}) - \mu_{im} c_{im} \quad (4)$$

where $Z = x/L$ (L is the depth of the sampling tube, the breakthrough data for which are being fitted with the model); $T = vt/L$; $P = v_m L/D_m$ is the Peclet number; $R = 1 + \rho_b K_d/\theta$ reflects retardation due to adsorption; $\beta = (\theta_m + f\rho_b K_d)/(\theta + \rho_b K_d)$ is the fraction of solute "sites" (water volume plus adsorption sites) in the mobile region; $\omega = \alpha L/\theta v$ is the scaled mass transfer coefficient; and $\mu_m = (\theta_m \mu_{l,m} + f\rho_b K_d \mu_{s,m})L/\theta v$ and $\mu_{im} = (\theta_{im}\mu_{l,im} + (1-f)\rho_b K_d \mu_{s,im})L/\theta v$ are scaled aggregate decay constants for the mobile and immobile regions, respectively. For an unreactive solute, $R = 1$, $\beta = \theta_m/\theta$, and μ_m and μ_{im} both vanish. In this work, the program CXTFIT v.2.1 (*17*) was used to fit these equations to breakthrough data obtained in experiments designed to approximate the following initial and boundary conditions: and

$$(1)\ c_m(Z,0) = c_{im}(Z,0) = 0 \text{ for all } Z \quad (5)$$

$$(2)\ c_m(0,T) - (1/P)\,\partial c_m(0,T)/\partial Z = c_i(T) = c_i \quad (6)$$

$$(3)\ \partial c_m/\partial Z(1,T) = 0 \quad (7)$$

where the input function $c_i(T)$ represents a 66 min pulse of solute-bearing solution of constant concentration c_i sprayed onto the top of the column (see Experimental Procedures). For the relationship between condition 2 and mass balance and the assumptions involved in condition 3, see the experimental work published by Parker and van Genuchten (*18*).

RESULTS AND DISCUSSION

Bromide Transport. Figure 2 shows bromide breakthrough data and fitted curves for sampling depths of 4−40 cm. The unreactivity of Br^- was confirmed by the total amount passing each sampling point, as calculated from the measured concentrations, sample volumes, and total flow rate, being on average 98% of the original Br^- pulse minus the quantities extracted in samples at lesser depths. For all of these curves, $R^2 > 0.99$, showing that the two-region model is capable of explaining the data.

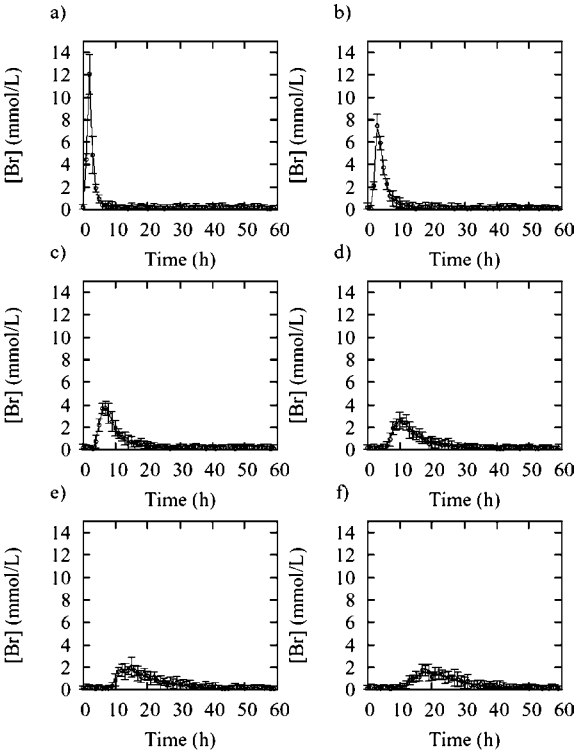

Figure 2. Concentration of bromide in samples taken from the column hourly at depths of 4, 8, 16, 24, 32, and 40 cm (a–f, respectively), together with the curves fitted in accordance with a two-region transport model. SEMs are shown by error bars.

Table 1 lists the values of β, Pe (Peclet number), and ω fitted for each depth L, together with those of v_m, which was optimized for each sampling depth starting from an initial value $v_m = v$, those of $D = D_m v/v_m$ (the global hydrodynamic coefficient of dispersion, calculated from the fitted value of Pe), and those of the dispersivity ($\lambda = D/V$). The depthwise increase in D and in the λ can be attributed to the scale-associated increase in the heterogeneity of pore size (which accordingly must increase particularly rapidly at depths shallower than 8 cm). However, because the increase in dispersivity is not proportional to depth but much slower (probably because of the narrow size range of the aggregates with which the soil column was constructed), it is insufficient to prevent the Peclet number from increasing from a value of 8 indicative of largely diffusive transport at $L = 4$ cm to a value of 56 indicative of convective transport at $L =$ 48 cm.

The value of β, 0.69 ± 0.022, indicates that the mobile water region predominated in the column, and the average value of α obtained from ω, $(2.55 \pm 2.51) \times 10^{-3}$ h^{-1}, that transfer of bromide to the immobile water region was very slow;that is, bromide was predominantly transported down preferential flow paths.

Endosulfan Transport. The breakthrough data for endosulfan show it to have been transported down the column in two waves: a fast wave reaching a depth of 40 cm after about 400 h and a very slow wave that by the time the experiment was terminated had only advanced some 8 cm (**Figure 3**). This

Table 1. Transport Parameters Obtained for a Two-Region Model of the Passage of Bromide through a Column of Vineyard Soil Aggregates

L (cm)	v_m (cm h^{-1})	D (cm^{2}h^{-1})	Pe	β	ω	λ (cm)	α (h^{-1})
4	1.610 ± 0.006	0.860 ± 0.042	7.5 ± 0.35	0.660 ± 0.009	0.042 ± 0.002	0.53 ± 0.024	7.52 10^{-3} ± 1.08 10^{-3}
8	1.630 ± 0.004	0.990 ± 0.033	13.2 ± 0.43	0.690 ± 0.006	0.047 ± 0.002	0.61 ± 0.019	4.26 10^{-3} ± 3.68 10^{-4}
16	1.635 ± 0.004	1.130 ± 0.026	23.2 ± 0.53	0.690 ± 0.005	0.048 ± 0.003	0.69 ± 0.014	2.18 10^{-3} ± 1.86 10^{-4}
24	1.647 ± 0.002	1.190 ± 0.018	33.2 ± 0.50	0.710 ± 0.004	0.042 ± 0.004	0.72 ± 0.010	1.28 10^{-3} ± 6.42 10^{-5}
32	1.658 ± 0.002	1.220 ± 0.016	43.5 ± 0.57	0.690 ± 0.006	0.044 ± 0.005	0.74 ± 0.009	1.01 10^{-3} ± 4.92 10^{-5}
40	1.662 ± 0.001	1.340 ± 0.015	49.6 ± 0.55	0.710 ± 0.008	0.046 ± 0.005	0.81 ± 0.009	8.51 10^{-4} ± 2.10 10^{-5}
48	1.683 ± 0.001	1.430 ± 0.015	56.5 ± 0.59	0.730 ± 0.009	0.043 ± 0.006	0.85 ± 0.008	7.52 10^{-4} ± 1.80 10^{-5}

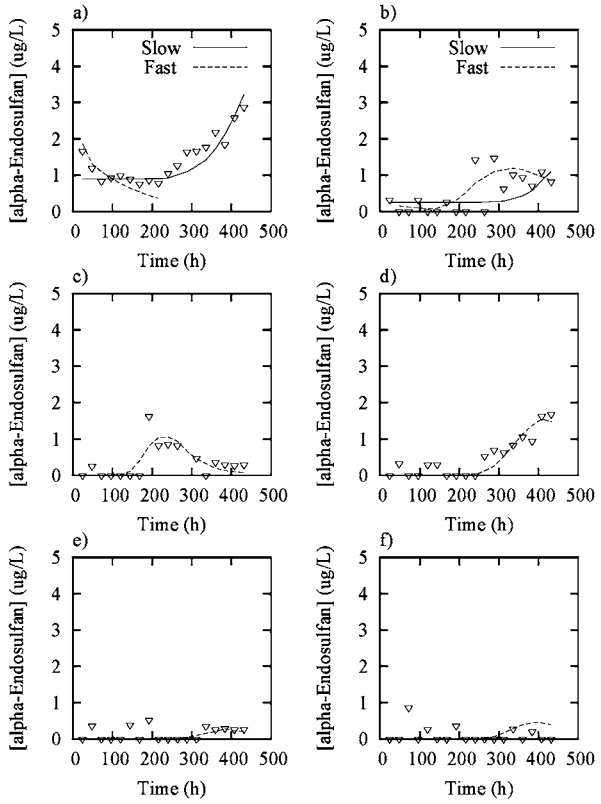

Figure 3. Concentration of endosulfan in samples taken from the column daily at depths of 4, 8, 16, 24, 32, and 40 cm (a–f, respectively). Curves were fitted as described in the Discussion.

behavior cannot be modeled by eqs 1 and 2, and therefore, to the extent that these equations suffice to model the existence of preferential flow paths, cannot be attributed solely to the existence of such paths.

Because Fosulan is an emulsion stabilized with surfactant, we first investigated whether the two-front behavior might be explained by distinguishing between emulsified and free endosulfan. According to this hypothesis, the fast front would reflect the transport of the micelles of the emulsion and the slow front the transport of extramicellar endosulfan capable of interacting with the soil matrix; the distinction between mobile and immobile regions was ignored. To test this hypothesis, we used the program CHAIN (*19*) to simulate the transport of intra- and extramicellar endosulfan assuming the latter to be derived from the former by a first-order process with rate constant k_L. In trials with various values of k_L and of the retardation factors R for intra- and extramicellar endosulfan, it was impossible to reproduce the observed behavior. Small k_L (0.001 h^{-1}) led to a single rapid breakthrough wave with an endosulfan content very much in excess of the observed values; large k_L (0.1 h^{-1}) suppressed the fast wave completely due to the adsorption of rapidly released endosulfan onto the soil, and no intermediate value was able to generate two well-separated waves of the required magnitude.

A previously published work using lysimeter and soil core analysis in Ustox soils (*20*) showed that endosulfan and other pesticides were rapidly transported to 40 cm soil depths regardless of their sorption properties, suggesting that leaching was caused by preferential flow. We therefore turned to a new hypothesis that recognized the existence of preferential flow paths shown by the analysis of the bromide data but also included other features to account for the two-wave transport behavior of endosulfan. According to this hypothesis, the fast and slow waves may be considered as corresponding to transport of two different endosulfan species (emulsified and free) that do not significantly interconvert in either direction. Neither of these species is significantly adsorbed in the mobile region ($f = 0$), and in the immobile region, once adsorbed reversibly, both are susceptible to a first-order process that makes their adsorption irreversible, i.e.

$$\mathrm{SE} \overset{K_d}{\longleftrightarrow} \mathrm{RAE} \overset{\mu}{\rightarrow} \mathrm{IAE}$$

where SE, RAE, and IAE are, respectively, solubilized, reversibly adsorbed, and irreversibly adsorbed endosulfan (which includes biological and/or chemical degradation of endosulfan).

We tested this hypothesis by fitting the two-region CXTFIT model independently to data for the fast and slow breakthrough waves. Under the above assumptions, eqs 1 and 2 reduce to

$$\theta_m \partial c_m/\partial t = \theta_m(D_m \partial^2 c_m/\partial x^2 - v_m \partial c_m/\partial x) - \alpha(c_m - c_{im}) \quad (8)$$

$$(\theta_{im} + \rho_b K_d) \partial c_{im}/\partial t = \alpha(c_m - c_{im}) - \rho_b K_d \mu c_{im} \quad (9)$$

and eqs 3 and 4 reduce to

$$\beta R \partial c_m/\partial T = (1/P) \partial^2 c_m/\partial Z^2 - \partial c_m/\partial Z - \omega(c_m - c_{im}) \quad (10)$$

$$(1 - \beta) R \partial c_{im}/\partial T = \omega(c_m - c_{im}) - \mu_2 c_{im} \quad (11)$$

where $\mu_2 = \rho_b K_d \mu L/\theta v$. With boundary and initial conditions equivalent to eqs 5−7, eqs 10 and 11 were fitted to the fast wave (mobile region) data for depths of 16 and 24 cm (**Figure 3c**,**d**) and to the 4 cm data for times greater than 150 h (**Figure 3a**), these latter being assumed to correspond solely to the slow wave (immobile region). In all three fits, the values of D, β, and α obtained in the analysis of the bromide experiments were imposed [β was imposed because leaving it as an adjustable parameter led to fitted values with a dispersion so large (0.120−0.999) as to make the mean meaningless and α because leaving it adjustable afforded no improvement in overall fit]. The remaining data in **Figure 3** were fitted "manually" by means

Table 2. Transport Parameters Obtained for Transport of Endosulfan through the Preferential Flow Region of a Column of Vineyard Soil Aggregates

L (cm)	R	K_d (L kg^{-1})	μ_2	μ (h^{-1})	$t_{0.5}$ (h)	R^2
4	7	2.06	2.24	1.040	0.67	0.56
8	25	8.25	8.41	0.098	7.07	0.93
16	27	9.94	9.11	0.031	22.6	0.83
24	29	9.63	9.81	0.051	13.7	0.83
32	20	6.53	6.66	0.053	12.9	0.32
40	15	4.81	4.91	0.073	9.6	0.49
48	15	4.81	4.91	0.066	10.5	0.27

Table 3. Transport Parameters Obtained for Transport of Endosulfan through the Nonpreferential Flow Region of a Column of Vineyard Soil Aggregates

L (cm)	R	K_d (L kg^{-1})	μ_2 ($\times 10^4$)	μ (h^{-1})	$t_{0.5}$ (h)	R^2
4	2121	729	70	2.6	267	0.896
8	740	254	50	1.0	693	0.899
16	1220	419	49	0.9	770	0.828
24	200	68	49	0.8	866	0.828

of a series of simulations in which various parameter values were used that were similar to those fitted as just described.

Tables 2 and **3** list, for the fast and slow endosulfan species, respectively, the values of the dimensionless parameters R and μ_2 obtained as described above, together with those of the corresponding dimensional parameters (K_d and μ), the half-life $t_{0.5}$ of the irreversible adsorption process, and the coefficients of determination of the fit, R^2. Whereas the values of K_d for the slow endosulfan species, 68−729 L/kg, are in the range reported by other authors (*5*, *21*−*24*), those obtained for the fast species are much lower, 2−10 L/kg.

In conclusion, the observed characteristics of the passage of commercial emulsified endosulfan through a column of vineyard soil under continual light simulated rain are adequately explained by a model in which passage takes place via both a preferential flow and a nonpreferential flow region; transfer between one region and the other is very slow; partition between soil and soil solution depends on the flow regime; and initial reversible adsorption is followed by a process that converts it in irreversible. These findings may account for both the presence of endosulfan in groundwater and its high persistence in soil. They imply that commercial endosulfan should not be applied to vineyards when soil humidity is such as to favor the formation and maintenance of preferential flow paths. The volumetric water content θ was measured as 0.445. This water content is near saturation, which implies that large pores are water filled, and this favors the preferential transport of endosulfan.

LITERATURE CITED

(1) Lode, O.; Eklo, O. M.; Holen, B.; Svensen, A.; Johnsen, A. M. Pesticides in precipitation in Norway. *Sci. Total Environ.* **1995**, *160/161*, 421−431.

(2) Ueoka, M.; Allinson, G.; Kelsall, Y.; Graymore, M.; Stagnitti, F. Environmental fate of pesticides used in Australian viticulture: behavior of dithianon and vinclozolin in the soils of the south Australian riverland. *Chemosphere* **1997**, *35*, 2915−2924.

(3) Fatoki, O. S.; Awofolu, R. O. Methods for selective determination of persistent organochlorine pesticide residues in water and sediments by capillary gas chromatography and electron-capture detection. *J. Chromatogr.* **2003**, *983* (1−2), 225−236.

(4) Wan, M. T.; Szeto, S.; Price, P. Distribution of endosulfan residues in the drainage waterways of the Lower Fraser Valley of British Columbia. *J. Environ. Sci. Health, Part B* **1995**, *30*, 401−433.

(5) Antonious, G. F.; Byers, M. E. Fate and movement of endosulfan under field conditions. *Environ. Toxicol. Chem.* **1997**, *16* (4), 644−649.

(6) Muller, J. F.; Duquesne, S. N. J.; Shaw, G. R.; Krrishnamohan, K.; Manonmanii, K.; Hodge, M.; Eaglesham, G. K. Pesticides in sediments from Queensland irrigation channels and drains. *Mar. Pollut. Bull.* **2000**, *41* (7), 294−301.

(7) Raupach, M. R.; Briggs, P. R.; Ford, P. W.; Leys, J. F.; Muschal, M.; Cooper, B.; Edge, V. E. Endosulfan transport: I. Integrative assessment of airborne and waterborne pathways. *J. Environ. Qual.* **2001**, *30* (3), 714−728.

(8) Schulz, R.; Peall, S. K. C.; Dabrowski, J. M.; Reinecke, A. J. Spray deposition of two insecticides into surface waters in a South African Orchard area. *J. Environ. Qual.* **2001**, *30* (3), 814−822.

(9) Cerejeira, M. J.; Viana, P.; Batisita, S.; Pereira, T.; Silva, E.; Valerio, M. J.; Silva, A.; Ferreira, M.; Silva-Fernandes, A. M. Pesticides in Portuguese surface and groundwaters. *Water Res.* **2003**, *37* (5), 1055−1063.

(10) Rial-Otero, R.; Cancho-Grande, B.; Arias-Estévez, M.; López-Periago, E.; Simal-Gándara, J. Procedure for the measurement of soil inputs of plant-protection agents washed off through vineyard canopy by rainfall. *J. Agric. Food Chem.* **2003**, *51*, 5041−5046.

(11) Ismail, B. S.; Enoma, A. O. S.; Cheah, U. B.; Lum, K. Y.; Malik, Z. Adsorption, desorption, and mobility of two insecticides in Malaysian agricultural soil. *J. Environ. Sci. Health.* **2002**, *B 37* (4), 355−364.

(12) Lennartz, B. Variation of herbicide transport parameters within a single field and its relation to water flux and soil properties. *Geoderma* **1999**, *91*, 327−345.

(13) Flury, H.; Flühler, H.; Jury, W. A.; Leuenberger, J. Susceptibility of soils to preferential flow of water: A field study. *Water Resour. Res.* **1994**, *30* (7), 1945−1954.

(14) Ghodrati, M.; Jury, W. A. A field study using dyes to characterize preferential flow of water. *Soil Sci. Soc. Am. J.* **1990**, *54*, 1558−1563.

(15) Thomas, L. C.; Chamberlin, G. J. *Colorimetric Chemical Analytical Methods*, 9th ed.; The Tintometer Ltd.: England, 1980.

(16) van Genuchten, M. Th.; Wagenet, R. J. Two-site/Two-region models for pesticide transport and degradation: Theoretical development and analytical solutions. *Soil Sci. Soc. Am. J.* **1989**, *53*, 1303−1310.

(17) Toride, N.; Leij, F. J.; van Genuchten, M. Th. *The CXTFIT Code for Estimating Transport Parameters from Laboratory or Field Tracer Experiments*, Version 2.1; Research Report no. 137; U.S. Salinity Laboratory, Agricultural Research Service, U.S. Department of Agriculture: Riverside, California, 1999; p 119.

(18) Parker, J. C.; van Genuchten, M. Th. Flux-averaged and volume-averaged concentrations in continuum approaches to solute transport. *Water Resour. Res.* **1984**, *20*, 866−872.

(19) van Genuchten, M. Th. Convective-dispersive transport of solutes involved in sequential first-order decay reactions. *Comput. Geosci.* **1985**, *11* (2), 129−147.

(20) Laabs, V.; Amelung, W.; Pinto, A.; Zech, W. Fate of pesticides in tropical soils of Brazil under field conditions. *J. Environ. Qual.* **2002**, *31*, 256−268.

(21) Ghadiri, H.; Rose, C. W. Endosulfan degradation in cotton farm soils. In *Minimizing the Impact of Pesticides on the Riverine Environment Using the Cotton Industry as a Model*; Second Annual Workshop; LWRRDC: Brisbane, Australia, 1994.

(22) Awasthi, N.; Manickam, N.; Kumar, A. Biodegradation of endosulfan by a bacterial co culture. *Bull. Environ. Contam. Toxicol.* **1997**, *59*, 928−934.
(23) Kathpal, T. S.; Singh, A.; Dhankhar, J. S.; Singh, G. Fate of endosulfan in cotton soil under subtropical conditions of Northern India. *Pestic. Sci*. **1997**, *50*, 21−27.
(24) Kaur, I.; Mathur, R. P.; Tandon, S. N.; Dureja, P. Persistence of endosulfan (technical) in water and soil. *Environ. Technol*. **1998**, *19*, 115−119.

Received for review March 10, 2005. Revised manuscript received June 23, 2005. Accepted June 24, 2005. This work was supported by the Xunta de Galicia and the Spanish Ministry of Science and Technology under Projects PGIDIT03PXIB38302PR and AGL2003-02244, respectively. B.C.-G. also thanks the Xunta de Galicia for a Parga-Pondal research grant, and M.A.-E. and E.L.-P. thank the Ministry of Science and Technology for Ramón y Cajal research contracts.

JF050545I